

A Group of Red, $\text{Ly}\alpha$ Emitting, High Redshift Galaxies¹

Paul J. Francis

University of Melbourne, School of Physics, Parkville, Victoria 3052, Australia
e-mail pfrancis@physics.unimelb.edu.au

Bruce E. Woodgate

NASA Goddard Space-Flight Center, Code 681, Greenbelt, MD 20771
e-mail woodgate@uit.dnet.nasa.gov

and

Anthony C. Danks

Hughes STX, Goddard Space-flight Center, Code 683.0, Greenbelt, MD 20771
e-mail danks@iue.gsfc.nasa.gov

ABSTRACT

We have discovered two new high redshift ($z = 2.38$) galaxies, near the previously known $z = 2.38$ galaxy 2139–4434 B1 (Francis et al. 1996).

All three galaxies are strong $\text{Ly}\alpha$ emitters, and have much redder continuum colors ($I - K \sim 5$) than other optically-selected high redshift galaxies. We hypothesize that these three galaxies are QSO IIs; radio-quiet counterparts of high redshift radio galaxies, containing concealed QSO nuclei. The red colors are most easily modelled by an old (> 0.5 Gyr), massive ($> 10^{11} M_{\odot}$) stellar population. If true, this implies that at least one galaxy cluster of mass $\gg 3 \times 10^{11} M_{\odot}$ had collapsed before redshift five.

Subject headings: galaxies: clusters: individual (2139–4434) — galaxies: distances and redshifts

¹Based on observations carried out at the Anglo Australian Telescope, Cerro Tololo Interamerican Observatory, and Siding Spring Observatory

1. Introduction

The first substantial samples of radio-quiet, high redshift ($z > 2$) galaxies are now being assembled (eg. Steidel et al. 1996, Lanzetta et al. 1996, Lowenthal et al. 1997). These galaxies have blue continuum colors (longward of the $\text{Ly}\alpha$ forest absorption), probably due to ongoing star formation. In contrast, many high redshift radio galaxies have very red continuum colors (eg. McCarthy 1993, Dunlop et al. 1996).

Recently, a small number of radio-quiet high redshift galaxies have been found which share the red colors of high redshift radio galaxies. Francis et al. (1996, hereafter F96) identified a very red radio-quiet $\text{Ly}\alpha$ -emitting galaxy (2139–4434 B1) at redshift 2.38, associated with a cluster of QSO absorption-line systems (Francis & Hewett 1993, hereafter FH93). Hu & Ridgway 1994 also identified a small number of extremely red sources, at least one of which is a radio-quiet high redshift galaxy (Graham & Dey 1996). If additional red, radio-quiet high-redshift galaxies were found, it would imply that the distinctively red colors of high redshift radio galaxies are not caused by the radio jets, and hence might be common in the early universe.

In this letter, we present the results of a search for more $\text{Ly}\alpha$ -emitting galaxies in the field around 2139–4434 B1. We assume $H_0 = 100h_{100}\text{km s}^{-1}\text{Mpc}^{-1}$, $h_{100} = 0.75$ (except where stated) and $q_0 = 0.5$.

2. Observations

The field around 2139–4434 B1 was searched for $\text{Ly}\alpha$ -emitting galaxies by imaging through a narrow-band filter tuned to a central wavelength of 411.6 nm, the expected wavelength of $\text{Ly}\alpha$ emission at B1’s redshift ($z=2.38$). Images were obtained on the night of 1995 October 27th, using a $2\text{k}\times 2\text{k}$ backside thinned CCD of the original HST/STIS (Space Telescope Imaging Spectrograph) design built by SITe, and installed in a Photometrics designed camera mounted at the prime focus of the Anglo-Australian Telescope (AAT). The doublet image corrector gave a field of view $11.7'$ on a side, which was centered midway between the two background QSOs described in FH93. Offband images were obtained through a B filter; exposure times were 5400 seconds in the narrow-band and 3600 seconds in the broad-band. A narrow-band surface brightness limit of $5.0 \times 10^{-20} \text{ W m}^{-2}\text{arcsec}^{-2}$ ($5.0 \times 10^{-17}\text{erg cm}^{-2}\text{s}^{-1}\text{arcsec}^{-2}$) was achieved (5σ), corresponding to a flux limit of $9 \times 10^{-20} \text{ W m}^{-2}$ ($9 \times 10^{-17}\text{erg cm}^{-2}\text{s}^{-1}$) for unresolved sources (seeing was $1.4''$); the filter passband width was 6.4 nm, corresponding to a redshift range of $\Delta z = 0.05$. The B -band image reached a (5σ) limiting magnitude of 25.8 for unresolved sources. After removal of

cosmic rays and bad pixels, the effective area surveyed was 70 square arcmin.

Four candidate Ly α emitting galaxies were detected, with excess narrow-band fluxes requiring an emission-line of rest-frame equivalent width > 10 nm (3σ). These included F96’s narrow-band excess sources B1 and B2, but their marginal candidate B3 was not confirmed.

Confirmation spectroscopy was obtained with the Low Dispersion Survey Spectrograph (LDSS) on the AAT, on the nights of August 13th and 14th 1996. A slit mask was designed to include all four candidates, with spare slits placed over lower priority candidates. A total of 47,700 seconds exposure was obtained, in $1.2''$ seeing, the the slits aligned with a position angle of 340° . The wavelength range covered spanned Ly α to He II at rest-frame $z=2.38$, with a resolution of 700km s^{-1} .

A deep R -band image of the field was obtained with the prime focus CCD at the CTIO 4-m telescope on October 19th 1995; exposure time was 4200 sec, and a (5σ) limiting magnitude of 25.5 was reached. Deep I -band imaging was obtained with LDSS on the AAT on November 11th 1996, reaching magnitude 24.4 in $1''$ seeing. Optical photometric calibration was obtained on 1995 August 16th with the Siding Spring 1-m telescope. The K_n imaging of F96 was extended with the CASPIR camera on the Siding Spring 2.3-m telescope, on August 12th and 13th 1995. The positions of all candidates were checked against the 13 cm and 20 cm radio maps of F96; none of the candidates are detected at a flux level of 0.27 mJy at either frequency. J , H and H α measurements were made from the data in F96.

3. Results

In addition to the previously confirmed B1, we detected C IV (154.9 nm) emission in F96’s second candidate galaxy B2, thus confirming its redshift. We did not detect their marginally significant candidate B3, but we found and confirmed a new Ly α source B4, for which we detect Ly α , C IV, He II (164.0 nm), and (with 2σ confidence) H α . The spectra are shown in Fig 1. None of the other sources were high redshift galaxies.

The properties of these three confirmed Ly α emitting galaxies at $z = 2.38$ are listed in Table 1, and their spectral energy distributions are shown in Fig 2. The redshifts of all three galaxies agree with each other, and with the redshift of FH93’s absorption-line cluster to within $\sim 600\text{km s}^{-1}$, and all lie within one square arcmin ($1'' \sim 5\text{kpc}$ in proper coordinates). The galaxies thus form a group of size ~ 1 Mpc; if they were randomly distributed in the surveyed volume the probability of finding them so close would only be

10^{-5} .

Fig 2 shows that all three Ly α galaxies have extremely red colors, even after the removal of Ly α and H α line emission from the B and K bands. B4 is spatially unresolved in all bands, but both B1 and B2 are marginally spatially resolved in the K-band; we defer a discussion of their morphologies pending upcoming Hubble Space Telescope observations.

4. Discussion

4.1. Emission-lines

Our galaxies have much stronger UV line emission than most of those of Steidel et al. (1996). Several pieces of evidence suggest that this strong line emission is powered by photoionization from active nuclei, and not by young stars. The strength of the high ionization lines (C IV and He II) is similar to that seen in radio galaxies, and implies that the emission-line gas is exposed to a hard ionizing continuum. The Ly α equivalent widths are close to the maximum that can be explained by stellar ionization (Charlot & Fall 1993). In B1 the Ly α emission comes from a much more extended region than the continuum emission (F96), and in B2, both the Ly α and C IV emission are displaced along the spectrograph slit away from the continuum source by $\sim 2''$ (~ 10 kpc). This suggests that the ionization source is physically separated from the emission-line region, which is most easily explained if the former is an active nucleus.

These Ly α sources are not however conventional QSOs: their Ly α equivalent widths (> 10 nm rest-frame) are higher than those of typical QSOs (~ 5 nm, Francis 1993), their velocity widths ($< 1500\text{km s}^{-1}$) are narrower than those of typical QSOs ($\sim 5000\text{km s}^{-1}$, Francis, Hooper & Impey 1993), and their continuum slopes are much redder ($B - K > 5$) than those of typical QSOs ($B - K \sim 2.5$, Francis 1996). The Ly α fluxes are however typical of the *extended* line emission around some high redshift quasars (eg. Heckman et al. 1991) and radio galaxies (McCarthy 1993). We therefore suggest that these three galaxies contain QSO IIs; radio-quiet active nuclei, which are concealed from our line of sight, perhaps by a dusty torus, ie. high redshift analogues of Seyfert II galaxies. Ionizing radiation from the concealed active nucleus does not reach us, but ionizes part of the gaseous environment of the host galaxy. If our sources have the same ratio of extended Ly α flux to continuum flux found in Heckman et al.'s (1991) sample of radio-loud quasars, the unobscured active nucleus would have an absolute B magnitude of ~ -24 ; ie. typical of weak QSOs, rather than Seyfert galaxies. This should be regarded as a lower limit to the QSO luminosity, as radio-quiet QSOs typically produce no detectable extended Ly α emission.

In both B1 and B2, the emission-line spectra (Fig 1) were obtained $> 1''$ from the continuum emission. For B1 the slit passed through the peak of the $\text{Ly}\alpha$ emission, which lies $\sim 1.5''$ to the SW of the continuum source (F96), and no continuum emission is seen in the spectrum. For B2, the $\text{Ly}\alpha$ and C IV emission were displaced $\sim 1''$ to the north of the top of the continuum emission, itself extended and clearly seen in the spectrum. The observed velocity widths of $\text{Ly}\alpha$ in both sources ($\sim 500 \text{ km s}^{-1}$) cannot, therefore, be due to the motion of emission-line clouds in the potential of a central black hole. If the gas is in virial equilibrium with the host galaxy mass, we derive host galaxy masses of $\sim 10^{12} M_{\odot}$. If the host galaxies are not this massive, however, some form of $\sim 10 \text{ kpc}$ scale radio-quiet wind or jet, or motion of the gas in a massive cluster potential, is required to give the observed velocities.

4.2. Continuum Emission

All three of our galaxies have much redder optical/near-IR continuum colors than those of Steidel et al. (Fig 2). They are also much redder than the $\text{Ly}\alpha$ emitting galaxy discovered by Djorgovski et al. (1996); no near-IR photometry is published for the other known $\text{Ly}\alpha$ selected high redshift galaxies (eg. Lowenthal et al. 1991, Pascarelle et al. 1996). The high redshift galaxies studied by Malkan, Teplitz & McLean (1996) and Ellingson et al. (1996) also have bluer optical/near-IR colors. The colors of our galaxies are, however, typical of many high redshift radio galaxies (eg. Lilly 1989), though due to our narrow-band $\text{H}\alpha$ imaging, we can remove the (small) emission-line contribution to our continuum colors, which is important in some radio galaxies (eg. Eales et al. 1993). Our galaxies are not as red as those of Hu & Ridgway (1994).

The red colors of our galaxies could be explained in three ways: by an old stellar population, dust obscuration, or reddened AGN light. Previous studies demonstrate that it is very hard to discriminate between these possibilities solely on the basis of broad-band photometry (eg. Lilly 1989, Chambers & Charlot 1990, Bithell & Rees 1990, Graham & Dey 1996, Dunlop et al. 1996).

As both B1 and B2 are spatially extended in the K-band, any AGN contribution to their red colors must be scattered. Polarimetry and HST imaging will indicate if this is significant in any of our galaxies. If the observed continuum emission is due to starlight, the galaxies could, at one extreme, be forming stars at $\sim 10^4 M_{\odot} \text{ yr}^{-1}$, with substantial dust obscuration ($E(B - V) \sim 1$), or at the other extreme, be dust free, massive ($> 2 \times 10^{11} M_{\odot}$), and old ($> 1 \text{ Gyr}$). These limits were calculated using the spectral synthesis models of Bruzual & Charlot (1995, see Bruzual & Charlot 1993), and dust extinction law of Calzetti

et al. (1994).

Producing red, spatially extended AGN light requires fine-tuning of the scattering geometry and viewing angle, which makes the presence of three such galaxies somewhat unlikely. The strong Ly α flux also suggests that these galaxies are not very dusty, as Ly α photons are very easily destroyed by even moderate amounts of dust. We therefore tentatively suggest that the red colors of our galaxies are produced by an old stellar population. This would, however, require the formation of mass concentrations of $\gg 10^{12} M_{\odot}$ at redshifts above 5; hard to explain in most cosmological models (eg. Kashlinsky & Jiminez 1997).

5. A New Population of High Redshift Galaxies?

How common could red galaxies be at high redshifts? Their red colors and clustering suggest that they might be the ancestors of some low redshift elliptical galaxies. If an appreciable fraction of ellipticals completed the bulk of their star formation before $z \sim 5$, as suggested by observations at intermediate redshifts (eg. Schade et al. 1996), the co-moving space density of red galaxies at $z \sim 2$ could be much higher than the observed upper limits on the co-moving densities of radio- and Ly α emitting galaxies. The difference could be made up by a population of red galaxies without active nuclei, which would not be found in radio or emission-line surveys.

Are broad-band optical surveys such as that of Steidel et al. (1996) and the Hubble Deep Field capable of finding this hypothetical population of red high redshift galaxies without active nuclei? Consider a model in which half of all the high redshift galaxies with a given rest-frame V -band magnitude are blue (with the colors of the Steidel et al. galaxies) and half are red (with the colors of our galaxies). The ratio of observed-frame optical flux to rest-frame optical flux of the blue galaxies is an order of magnitude greater than that of the red galaxies. Thus to be included in a sample with a magnitude limit in the observed-frame optical, a red galaxy will have to be an order of magnitude more luminous in the rest-frame V -band than a blue galaxy. If the high redshift V -band luminosity function is similar to a Schechter function (Schechter 1976), the space density of the red galaxies in a optically magnitude limited sample will thus be only $\sim 10^{-4}$ that of blue galaxies. As current optically selected surveys have sizes of only $\sim 10^2$ galaxies, they would not therefore contain any red galaxies. Some recent IR selected galaxy surveys are, however, finding sources that could be red, high redshift galaxies (Moustakas et al. 1997).

In conclusion, we have detected a group of three radio-quiet high redshift galaxies with

strong emission-lines and red continuum colors. The emission-lines are probably caused by photoionization by a concealed radio-quiet active nucleus, while the red colors could be due to some combination of dust, scattered AGN light and an old stellar population. Equally red galaxies without active nuclei could be an important population in the high redshift universe.

We wish to thank Bob Dean, Karl Glazebrook, and all the staff at the AAT, for their able assistance, and Alistair Walker for obtaining the CTIO service imaging.

REFERENCES

- Bithell, M. & Rees, M. J. 1990, MNRAS, 242, 570
- Bruzual, A. G., & Charlot, S. 1993, ApJ, 405, 538
- Calzetti, D., Kinney, A. L., & Storchi-Bergmann, T. 1994, ApJ, 429, 582
- Chambers, K. C. & Charlot, S. 1990, ApJ, 348, L1
- Charlot, A., & Fall, S. M. 1993, in *First Light in the Universe*, ed. B. Rocca-Volmerange et al. (Gif-sur-Yvette: Ed. Frontières), 341
- Djorgovski, S. G., Pahre, M. A., Bechtold, J. & Elston, R. 1996, Nature, 382, 234
- Dunlop, J., Peacock, J. A., Spinrad, H. J., Dey, A., Jiminez, R., Stern, D. & Windhorst, R. 1996, Nature, 381, 581
- Eales, S., Rawlings, S., Puxley, P., Rocca-Volmerange, B. & Kuntz, K. 1993, Nature, 363, 140
- Ellingson, E., Yee, H. K. C., Bechtold, J., & Elston, R. 1996, ApJ, 466, L71
- Francis, P. J. 1993, ApJ, 405, 119
- Francis, P. J. 1996, 1996, Publ. ASA., 13, 212
- Francis, P. J., & Hewett, P. C. 1993, AJ, 105, 1633 (FH93)
- Francis, P. J., Hooper, E. J. & Impey, C. D. 1993, AJ, 106, 417
- Francis, P. J., Woodgate, B. E., Warren, S. J., Møller, P., Mazzolini, M., Bunker, A. J., Lowenthal, J. D., Williams, T. B., Minezaki, T., Kobayashi, Y., & Yoshii, Y. 1996, ApJ, 457, 490 (F96)
- Graham, J. R. & Dey, A. 1996, ApJ, 471, 720
- Heckman, T. M., Lehnert, M. D., van Breugel, W., & Miley, G. K. 1991, ApJ, 370, 78
- Hu, E. M. & Ridgway, S. E. 1994, AJ, 107, 1303
- Kashlinsky, A., & Jiminez, R. 1997, ApJ, 474, L81
- Lanzetta, K. M., Yahil, A. & Fernandez-Soto, A. 1996, Nature 381, 759
- Lilly, S. J. 1989, ApJ, 340, 77
- Lowenthal, J. D., Hogan, C. J., Green, R. F., Caulet, A., Woodgate, B. E., Brown, L., & Foltz, C. B. 1991, ApJ, 377, L73
- Lowenthal, J. D., Koo, D. C., Guzman, R., Gallego, J., Phillips, A. C., Faber, S. M., Vogt, N. P., Illingworth, G. D. & Gronwall, C. 1997, ApJ, in press
- Malkan, M. A., Teplitz, H. & McLean, I. S. 1996, ApJ, 468, L9

- McCarthy, P. J. 1993, *ARA& A*, 31, 639
- Moustakas, L. A., Davis, M., Graham, J. R., Silk, J., Peterson, B. A. & Yoshii, Y. 1997, *ApJ*, 475, 445
- Pascarelle, S. M., Windhorst, R. A., Driver, S. P., & Ostrander, E. J. 1996, *ApJ*, 456, L21
- Schade, D., Carlberg, R. G., Yee, H. K. C., Lopez-Crux, O., & Ellingson, E. 1996, *ApJ*, 464, 63
- Schechter, P. 1976, *ApJ*, 203, 297
- Steidel, C. C., Giavalisco, M., Pettini, M., Dickinson, M. & Adelberger, K. L. 1996, *ApJ*, 462, L17

Table 1. Galaxy Properties

	B1	B2	B4
RA (B1950) ^a	21:39:16.38	21:39:18.56	21:39:20.98
DEC (B1950) ^a	−44:34:12.2	−44:34:45.0	−44:34:00.8
Ly α Flux ($\times 10^{-19} \text{Wm}^{-2}$)	8.0 ± 0.5	2.1 ± 0.3	1.8 ± 0.3
Ly α Rest-frame Equivalent Width (nm)	22 ± 4	> 10	> 12
H α Flux ($\times 10^{-19} \text{Wm}^{-2}$)	9.2 ± 1.5	< 6.6	4.0 ± 1.4
Ly α /C IV	7	8	4.4
Ly α /He II	...	> 16	3.3
Ly α velocity width (FWHM, kms^{-1})	600 ^c	450 ^c	1200
Line-subtracted continuum colors			
<i>B</i>	25.9 ± 0.2	> 26.6	> 26.9
<i>R</i>	24.2 ± 0.1	24.8 ± 0.2	25.9 ± 0.5
<i>I</i>	23.8 ± 0.5	23.3 ± 0.5	24.3 ± 0.5
<i>J</i>	21.8 ± 0.2	22.0 ± 0.2	> 21.5
<i>H</i>	19.9 ± 0.3
<i>K</i>	19.0 ± 0.2	19.9 ± 0.3	19.1 ± 0.2

^aPosition is for the centroid of the Ly α flux.

^bUpper and Lower limits are 3σ .

^cMeasured from the higher resolution spectra of F96.

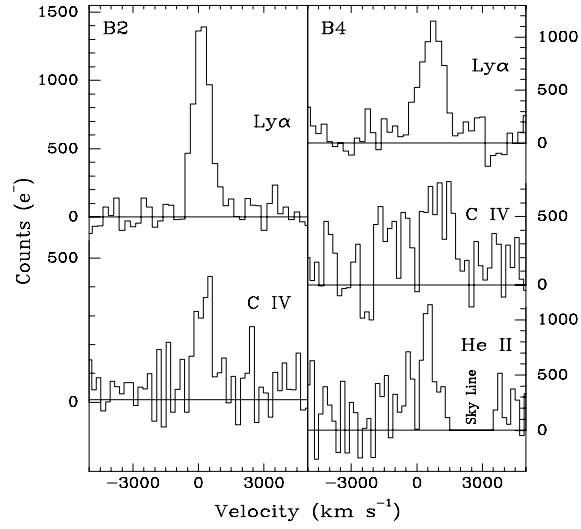


Fig. 1.— Spectra of B2 and B4. Velocities are relative to the centroid of the QSO absorption system in QSO 2139–4434, which is at 410.9 nm. Note that the red wing of He II is clearly separated from the sky line marked in the two-dimensional spectrum. The spectra have been sky subtracted but not rebinned or flux calibrated.

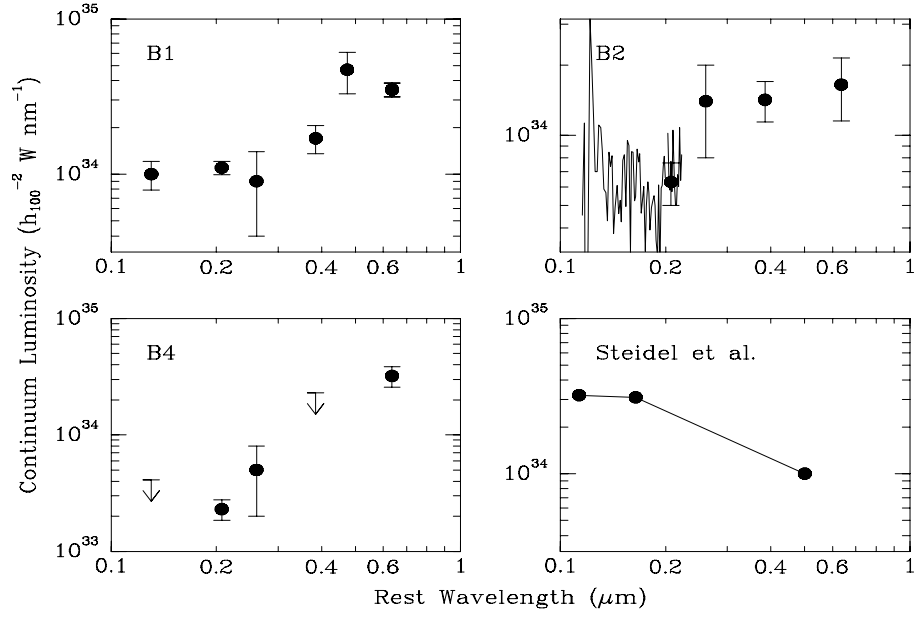


Fig. 2.— Continuum spectral energy distributions of the three Ly α galaxies, compared with a composite spectral energy distribution for the galaxies in Steidel et al. (1996) with listed K -band magnitudes. $1 \text{ W nm}^{-1} \equiv 10^6 \text{ erg s}^{-1} \text{ \AA}^{-1}$